HHS Public Access

Author manuscript

Opt Lett. Author manuscript; available in PMC 2019 March 22.

Published in final edited form as:

Opt Lett. 2016 July 15; 41(14): 3225–3228. doi:10.1364/OL.41.003225.

Enhanced detection of early photons in time-domain optical imaging by running in “dead-time” regime

LAGNOJITA SINHA[1], **JOVAN G. BRANKOV**[2], and **KENNETH M. TICHAUER**[1,*]

[1]Department of Biomedical Engineering, Illinois Institute of Technology, Chicago, IL 60616

[2]Department of Electrical and Computer Engineering, Illinois Institute of Technology, Chicago, IL 60616

Abstract

Optical tomography can yield anatomical and molecular information about biological tissue. However, its spatial resolution is poor in thick samples owing to high scatter. Early-photon approaches, where photon arrival times are measured with time-resolved detectors provide one means of improving spatial resolution through selection of photons that travel a straighter path. Here, a novel approach to significantly enhance detection of early photons in time-correlated single photon counting with avalanche photodiodes has been discussed. Results suggest that early photon detection rate can be increased by about 10 orders-of-magnitude by running detector in dead-time regime.

Keywords

(170.3890) Medical optics instrumentation; (170.6920) Time-resolved imaging; (170.6960) Tomography

Absorption and fluorescence-based optical tomography has been heralded as a low-cost, ionizing radiation-free alternative to conventional medical imaging modalities for decades, particularly for tissue specimen and small animal imaging [1, 2]. However, a major limitation to optical tomography is the highly scattering nature of photon propagation in biological tissue. This scattering obfuscates the ability to predict the exact path of a detected photon, effectively setting spatial resolution limits of approximately 1 mm [3]. One solution to improving spatial resolution is so-called early-photon tomography. Early photon tomography requires pulsed light sources and advanced time-resolved detection of the transmitted photons so that the earliest arriving photons, having taken the most direct path between source and detector, can be selectively isolated to improve reconstructed image spatial resolution. There are a number of ways to achieve early photon detection with time-resolved detectors [4–10]; this study presents a method to significantly enhance the detection rate of the earliest possible photons by running laser power high enough to ensure that time-correlated single photon counting (TCSPC) single photon avalanche photodiode (SPAD)

*Corresponding author: tichauer@iit.edu.

illumination is far above the count-rate that causes dead-time of the detectors. Henceforth, this will be referred to as the “dead-time regime.”

Through tissues thicker than 1 mm, the vast majority of photons reaching the detector in transillumination (light source and detector on opposite sides of the sample) mode will be diffuse photons, having taken an indirect path through the tissue. All photons will have some interaction with the tissue at this level; however, photons that tend to scatter in a forward direction and are not absorbed (very early-arriving or “forward scattering” photons), I_{fs}, can be estimated from the Beer-Lambert Law:

$$I_{fs}(l) = I_0 e^{-l(\mu_a + \mu_s)}, \quad (1)$$

where l is the diameter of the sample being imaged, μ_a and μ_s are the absorption and scattering coefficients of light in the tissue, respectively, and I_0 is the rate of photons emitted from the light source: typical values of μ_a and μ_s are 0.02 mm^{-1} and 10 mm^{-1}, respectively, in the near-infrared regime (700–900 nm) [11].

A comparative approximation of the rate of all photons reaching the detector in diffuse media can be estimated by the diffusion approximation to the radiative transfer equation [12]:

$$I_{all}(l) = I_0 \frac{3\mu_s(1-g)NA}{4\pi l} e^{-1\sqrt{3\mu_a(\mu_a + (1-g)\mu_s)}}, \quad (2)$$

where g is the anisotropy of the scatter and is generally considered to be approximately 0.9 for biological tissue [11], and NA is the numerical aperture of the detector. Assuming NA = 0.05, g = 0.9, μ_a = 0.02 mm^{-1}, and μ_s = 10 mm^{-1}, the proportion of detected photons that are forward-scattering as a function of sample thickness is:

$$\frac{I_{fs}(l)}{I_{all}(l)} = \frac{4\pi l}{3\mu_s(1-g)NA} e^{-l(\mu_a + \mu_s - \sqrt{3\mu_a(\mu_a + (1-g)\mu_s)})} = 27\pi l e^{-9.8l}. \quad (3)$$

Equation (3) estimates that through 1 mm tissue, as many as 1 in 200 near-infrared photons reaching the detector may be forward scattering, However, as tissue thickness increases, the exponential nature of Eq. (3) dominates, and by 4 mm, as few as 1 in 10^{14} photons reaching the detector are forward scattering. To identify rare forward scattering photons (the earliest arriving photons), one would require a detector with as fine a temporal resolution as possible. To date, the best temporal resolution is provided by time-correlated single photon counting (TCSPC) systems, typically using either photomultiplier tubes (PMTs) or SPADs to amplify the signal from a single photon event. However, conventional use of such systems has aimed to keep photon count-rates low enough to limit dead-time/”pile-up” effects (i.e., limiting the occurrence of more than one photon arriving at the detector within the duration of the dead-time of the system). By running these detectors in a sub-dead-time regime, the

far more abundant diffuse photons will swamp forward scattering and other very early arriving photons. This keeps count rates of these rare photons below typical background levels (Fig 1a), so that even with increased exposure, signal cannot be recovered.

Using relatively robust SPAD detectors rather than PMTs for TCSPC – the latter of which is sensitive to overheating damage with high photon incidence rates – can allow for use of higher-powered light sources. And while longer dead-time of these detectors also limits the maximum photon count rate to ~10^6 per second, as long as the inverse of the laser repetition rate is longer than the dead-time of the TCSPC system, the earliest arriving photons within each pulse period will be detected preferentially to any later arriving photons [13]. In other words, the use of SPAD-based TCSPC systems in a dead-time regime can provide a means to significantly enhance the number of detected early photons while the later arriving photons will become increasingly masked by the detector's dead-time as photon rate at the detector increases.

Temporally discriminating the extremely rare forward scattering photons may not be possible with current temporal resolution limitations in TCSPC; however, significant improvements in spatial resolution have been demonstrated by carrying out image reconstruction only on the photons in the earliest time gate possible [4–8]. So, while the preceding theoretical handling of the problem focused on forward-scattering photon statistics for simplicity, the principles can be scaled to the population of photons arriving within the earliest gate of the TCSPC system. Therefore, by exposing TCSPC detection systems to pulsed light sources that will far exceed the detection dead-time limit of the detector, many orders-of-magnitude improvement can be achieved in the probability of detecting photons arriving in the earliest detectable gates. The remainder of this letter explores these dead-time improvements in more detail through simulation and phantom experiments, demonstrating that the number of detected early photon remains linear at high laser power, and significant improvements in spatial resolution can be achieved by even marginally enhancing laser power.

Simulation Results.

The analytical solution of photon propagation through a 4-mm thick tissue was used to simulate a typical photon tissue-transit-time point-spread-function with reduced scattering coefficient $\mu_s' = 1\ \text{mm}^{-1}$ and absorption coefficient $\mu_a = 0.02\ \text{mm}^{-1}$ [12]. This solution was then scaled to various photon count rates in 4 ps time bins (matching the characteristics of the TCSPC system described below) by normalizing to power levels achievable experimentally with an LDH-PC780 pulsed-diode laser (PicoQuant, Berlin, Germany). The saturation and dead-time effect of the detector were implemented [14] with an assumption that the dead-time was 80 ns (comparable to the detector in our system described below). The table in Fig. 1b demonstrates that with increasing laser power, the rate of photons reaching the detector increased linearly; however, because of the dead-time effect, the maximum rate of photon detection saturated at about 5×10^5 photons/s assuming a laser pulse repetition rate of 5 MHz. The plots in Fig 1c demonstrate that the rate of photons detected will underestimate the rate of photons incident on the detector at higher laser powers, with photon count rates in later gates decreasing as governed by dead-time effect

principles [14]. Fig 1d demonstrates that with increasing power, the dead-time effect leads to an apparent shift in photon arrival time detection to earlier gates, thus boosting the probability of early photon detection at the expense of late arriving photon counting. This shift is not a true shift to earlier photons. In fact the shape of the photon arrival time distribution incident on the detector does not change, only the scale increases (dashed curve in Fig. 1c). It is rather the fact that the probability of detecting photons arriving in the early gates remains unchanged with laser power, while the probability of detecting the later-arriving photons diminishes significantly with increased laser power because of the dead-time of the detector.

Experimental Results.

The early photon system (Fig. 1e) consisted of a 785 ± 4 nm wavelength pulsed-diode laser (LDH-PC780, PicoQuant) powered by a laser driver (PDL 800-B, PicoQuant) illumination source pulsed at 5 MHz and at full power. The pulse width of this laser is approximately 100 ps (note: shorter pulsed lasers are available that could further enhance this dead-time regime methodology; however, this laser is sufficient for demonstrating the effect in principle). A 0–4 OD attenuator (Thorlabs, Newton, NJ) was used to control the power of the laser source incident on the scattering medium without changing the shape of the laser pulse. Laser power exiting the variable attenuator was monitored with a power meter (S120C, Thorlabs). A 5-mm diameter cuvette filled with 1% Intralipid® (Sigma-Aldrich, St. Louis, USA) and India ink (Winsor & Newton, London, UK) in water to match the optical properties of the simulations [11] was used as a phantom. Lenses (Thorlabs, Newton, NJ) were used for focusing the signal. The transmitted signal was then detected by a SPAD (PDM, PicoQuant) connected to a TCSPC module (PicoHarp 300, PicoQuant) to obtain temporal information at 4 ± 25 ps temporal resolution over the 200 ns pulse repetition period and with a dead-time of approximately 80 ns. The effective detector area of the SPAD was 50 × 50 μm2. The TCSPC system and laser driver were connected through a TTL port to reference the time of arrival of each photon to the nearest laser pulse. All control of the system was carried out with in-house software developed in MATLAB (Mathworks, Natick, MA).

Attenuation of the laser down to a power of 0.005 μW was needed to completely avoid dead-time effects at the detector. This occurs with this TCSPC approach when the inverse of the rate of photon detection is less than 5% of the duration of the dead time (~80 ns), capping the photon detection rate at approximately 2.5×10^5 photons/s. Increasing the laser power above this threshold triggered a warning on the built-in PicoHarp software, to notify the user that dead-time effects may be affecting photon count rates. Since the purpose of this study was to evaluate the effects of this dead-time in aiding detection of rare early photons, the variable attenuator was decreased to increase power over a range from 0.05 μW all the way up to 0.5 mW, which was the maximum power of the laser under the defined settings. It should be noted that this was well below the ANSI safety limit for skin, which is ~2 W for this wavelength and type of light source. With ANSI safety limits being conservative limits for *in vivo* human studies, it is conceivable that the laser power could be increased by up to 4 or 5 orders of magnitude (to observe thicker tissue) compared to what was used as a maximum power in the current study, further supporting the enormous potential of detecting early photons in a dead-time regime.

Fig. 2a demonstrates the saturation characteristics observed with dead-time in TCSPC match with what was predicted by simulations of dead-time (Fig. 1d); specifically, that early-gate photon count rates increase with increased laser power, while later-gate photon count rates decrease commensurately maintaining the total count rate below the saturation limit for all laser powers yielding photon incidence rates at the detector that exceed 1/dead-time. The saturation effect of the detector mainly affects the later gates of the TPSF, while the earliest gates are not affected. Moreover, as power increases from a range where all time bins are linear with power (detection rate < 5% of pulse rate), the likelihood of 1 or more photons arriving at the detector within the dead-time caused by detection of an earlier arriving photon, increases. Since these photons will not be counted, earlier photons will always be detected preferentially to later arriving photons at high fluence rates, keeping their linearity in response to photon fluence at the expense of later-arriving photon detection efficiency (Fig. 2b). Only at very high fluence rates, when close to 1 earliest-gate-photon arrives at the detector every pulse, will the linearity get affected in all gates.

To make the detector reach its saturation the laser needs to be ramped up and such high signal can cause an effect called afterpulsing in the detector. In saturation mode after the dead time is over the trapped carrier can generate a late signal, which decreases exponentially but can spread over a few microseconds, also called afterpulsing. However, results of TPSFs presented in Fig 2c in the dead-time regime and sub-dead-time suggest that even though afterpulsing increases at at higher intensities, it has no time correlation and be considered an offset in the signal. To correct for this offset of temporally uniform background, the average rate of afterpulse detection per bin can be estimated from regions of the TPSF far from the measured light pulse, and then subtracted from all bins in the TPSF.

Phantom Experiment Results.

For further analysis, Monte-Carlo simulation was used to test how much better resolution could be achieved if a certain time window was used for reconstruction [15]. Dead-time regime early gate photons were compared to conventional early gate photons – defined here as gates taken over a time span of 120 ps centred at 25% of the peak of the measured photon arrival distribution collected at a laser power below the detector dead-time regime[8, 16]. The sensitivity function at a detector at location r_d for a light source at r_s was obtained by convolving the time resolved Monte monte Carlo carlo (*MC*) simulation for a 4 mm x 4 mm x 4 mm sample with optical properties similar to tissue (μ_a = 0.02 mm^{-1} and μ_s = 10 mm^{-1}, g = 0.9) with the instrument response function (*IRF*) (Fig. 2d).

$$sensitivity(r_s, r_d, t) = \int_0^t MC(r_s, r_d, \tau) * IRF(t-\tau)d\tau\,. \quad (4)$$

Three inclusions were added to the sample of length 200 μm each having a higher absorption coefficient than the background ($\Delta\mu_a$ = 1 mm^{-1}) (Fig. 3c). Projection profiles were estimated by taking the product of the Monte-Carlo sensitivity photon likelihood path distributions through the sample (for dead-time regime early photons and conventional photons – Fig.

3a&b respectively) assuming adjacent source-detector positions to be ranging from −0.5–0.5 mm in the vertical direction.

Fig. 3d provides a preliminary demonstration of the resolution gains that can be obtained with dead-time regime early photons compared to conventional early photons. It should be noted that the Monte-Carlo was carried out with 5×10^8 photons, while ANSI safety limits would allow for far greater fluence in reasonable imaging times (a rate that is very time consuming to simulate with Monte-Carlo), and so the Monte-Carlo data here is likely to suffer from the same issues of inefficient photon detection rates in early gates as with conventional TCSPC detection discussed in the Introduction section. So, even in this very conservative estimate, getting the earliest gate photons in the dead-time regime can provide significant improvements on spatial resolution in diffuse optical tomography over conventional early photons. The experimental data (Fig. 3e) was well supported by the simulation. The phantom used was a 4 × 4 × 4 mm box filled with the lipid solution (μ_a = 0.02 mm^{-1} and μ_s‘ = 1 mm^{-1}) with centrally placed three bars having much higher absorption (μ_a ~= 8 mm^{-1}) separated by 200 μm, as in the simulation. The 4 mm width was specially selected such that significant saturation effects could be observed with the laser power (~ 1 mW) used in this first generation of this system. Wider samples will be explored with higher-powered laser sources in future; however, the work serves to demonstrate the principles of early photon detection enhancement through dead-time effects.

The signal to noise ratio (*SNR*) was computed by the following relation

$$SNR = \mu_{signal}/\sigma_{noise}, \quad (5)$$

where μ_{signal} is the average of the signal intensity while σ_{noise} is standard deviation of the noise in the image. The *SNR* was computed to be 100.56 using our approach while as low as 6.45 using the same bin in an unsaturated case, keeping in mind that a trade off exists between selection of early photon and higher noise level in the images.

In this letter, a first demonstration of a novel method to enhance detection of low-scattering, early-arriving photons in time-resolved diffuse optical tomography is presented. We showed that by running TCSPC detector in dead-time regime detection of early arriving photons can be maintained while only later arriving photons will be affected by dead-time. Our simulations suggest that up to 10 orders-of-magnitude improvements in early photon detection can be achieved through tissues thicker than a few millimeters. Furthermore, we demonstrate this phenomenon experimentally and through simulation, highlighting the fact that the earliest photons, once detected at rates higher than the background level, are detected in a linear fashion for a wide range of laser powers (and despite the severe nonlinearity of later-arriving photon detection in this regime). Finally, a preliminary simulation of the levels of spatial resolution improvement achievable in the dead-time regime early photons compared to conventional early photons is presented with an SNR improvement of almost 20 times, with the caveat that lasers of much higher power and narrower pulse width can be used to further enhance spatial resolution to match the many orders-of-magnitude improvements predicted by the analytical models.

Funding sources and acknowledgments.

This work was supported by start-up funds from the Illinois Institute of Technology, a Pilot Project Grant from the Pritzker Institute of Biomedical Science and Engineering, and from the Nayar Prize at Illinois Institute of Technology (Phase I).

References

1. Chugani HT, Phelps ME, and Mazziotta JC, “Positron emission tomography study of human brain functional development,” Annals of neurology 22, 487–497 (1987). [PubMed: 3501693]
2. Hachamovitch R, Berman DS, Shaw LJ, Kiat H, Cohen I, Cabico JA, Friedman J, and Diamond GA, “Incremental prognostic value of myocardial perfusion single photon emission computed tomography for the prediction of cardiac death: differential stratification for risk of cardiac death and myocardial infarction,” Circulation 97, 535–543 (1998). [PubMed: 9494023]
3. Arridge SR and Schotland JC, “Optical tomography: forward and inverse problems,” Inverse Probl 25(2009).
4. Bassi A, Brida D, D’Andrea C, Valentini G, Cubeddu R, De Silvestri S, and Cerullo G, “Time-gated optical projection tomography,” Optics letters 35, 2732–2734 (2010). [PubMed: 20717439]
5. Fieramonti L, Bassi A, Foglia EA, Pistocchi A, D’Andrea C, Valentini G, Cubeddu R, De Silvestri S, Cerullo G, and Cotelli F, “Time-gated optical projection tomography allows visualization of adult zebrafish internal structures,” PloS one 7, e50744 (2012). [PubMed: 23185643]
6. Leblond F, Dehghani H, Kepshire D, and Pogue BW, “Early-photon fluorescence tomography: spatial resolution improvements and noise stability considerations,” Journal of the Optical Society of America. A, Optics, image science, and vision 26, 1444–1457 (2009).
7. Niedre M and Ntziachristos V, “Comparison of fluorescence tomographic imaging in mice with early-arriving and quasi-continuous-wave photons,” Optics letters 35, 369–371 (2010). [PubMed: 20125724]
8. Niedre MJ, de Kleine RH, Aikawa E, Kirsch DG, Weissleder R, and Ntziachristos V, “Early photon tomography allows fluorescence detection of lung carcinomas and disease progression in mice in vivo,” Proceedings of the National Academy of Sciences of the United States of America 105, 19126–19131 (2008). [PubMed: 19015534]
9. Turner GM, Zacharakis G, Soubret A, Ripoll J, and Ntziachristos V, “Complete-angle projection diffuse optical tomography by use of early photons,” Optics letters 30, 409–411 (2005). [PubMed: 15762444]
10. Zhang B, Cao X, Liu F, Liu X, Wang X, and Bai J, “Early-photon fluorescence tomography of a heterogeneous mouse model with the telegraph equation,” Applied optics 50, 5397–5407 (2011). [PubMed: 22016206]
11. Jacques SL, “Optical properties of biological tissues: a review,” Physics in medicine and biology 58, R37–61 (2013). [PubMed: 23666068]
12. Durduran T, Choe R, Baker WB, and Yodh AG, “Diffuse Optics for Tissue Monitoring and Tomography,” Reports on progress in physics. Physical Society 73(2010).
13. Charbon E, Fishburn M, Walker R, Henderson RK, and Niclass C, “SPAD-Based Sensors,” In TOF Range-Imaging Cameras, pp 11–38. Springer Berlin Heidelberg (2013).
14. Gedcke DA, “Dealing with dead time distortion in time digitizer,” ORTEC Application Note AN57 (2001).
15. Fang Q and Boas DA, “Monte Carlo simulation of photon migration in 3D turbid media accelerated by graphics processing units,” Optics express 17, 20178–20190 (2009). [PubMed: 19997242]
16. Mu Y and Niedre M, “A fast SPAD-based small animal imager for early-photon diffuse optical tomography,” Conf Proc IEEE Eng Med Biol Soc 2014, 2833–2836 (2014). [PubMed: 25570581]

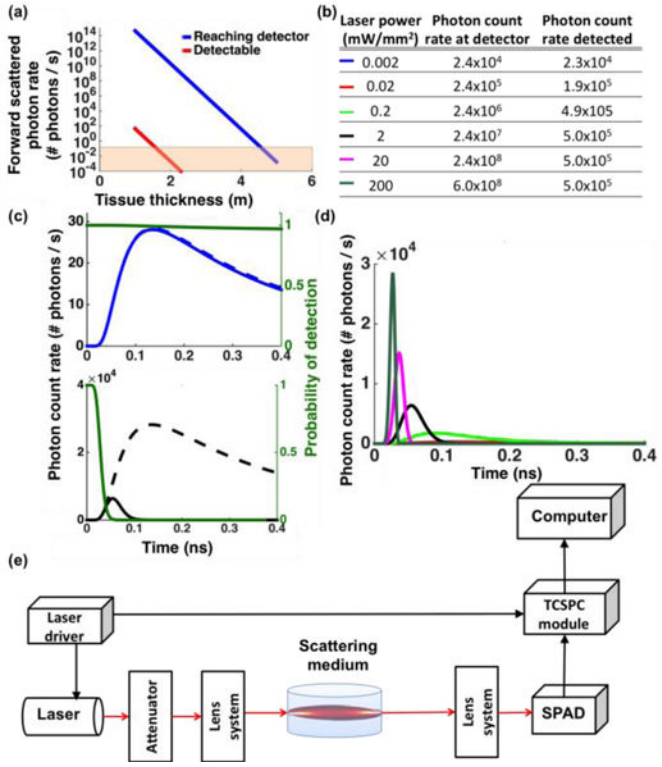

Fig. 1.

Effects of dead-time on time-resolved pulsed light detection. (a) Rate of forward scattered photons reaching the detector is presented when running the laser at the ANSI safety limit (blue curve: 10^{19} photons/s laser output) and at a power just below the dead-time regime threshold (red curve: 10^{7} photons/s laser output). The orange shaded region represents photon count rates below the background (populations that cannot be recovered by increased exposure time). (b) A relation between laser power, rate of photons hitting the detector, and rate of photons counted. (c) Simulated photon count rates as a function of arrival time just above the dead-time threshold (blue dashed curve – upper plot) and well above the dead-time threshold (black dashed curve – lower plot). The corresponding solid curves demonstrate how the dashed curve will be observed with dead-time saturation of later gates. The green curves demonstrate the probability of detecting a photon at the detector in a given time-bin. (d) Simulated photon counts for various power levels as shown in (b): note, all but the one corresponding to the 0.002 mW/ mm^2 power – blue curve – is affected by dead-time. (e) The schematic of the system.

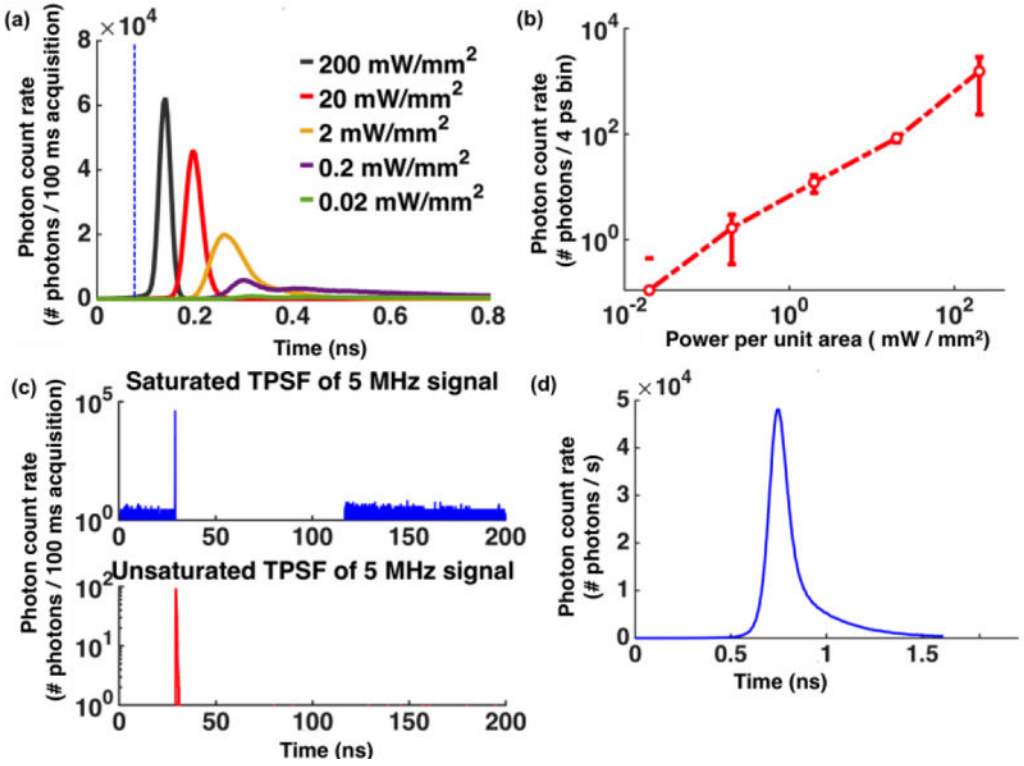

Fig. 2.

Experimental observations. (a) Change in shape of the pulses as the dead-time effect increases through increasing the laser power : can be compared to the simulation results in Fig. 1d. (b) A demonstration of the linearity between the early-gate photons (blue dashed line in (a) at t = 0.07 ± 0.016 ns) and laser power . (c) After-pulsing was observable for TPSFs collected in dead-time regime (saturated; blue data) but not for standard TPSFs (unsaturated; red data). (d) The instrument response function (IRF) of the system. The acquisition time of the detector for each measurement was 100 ms.

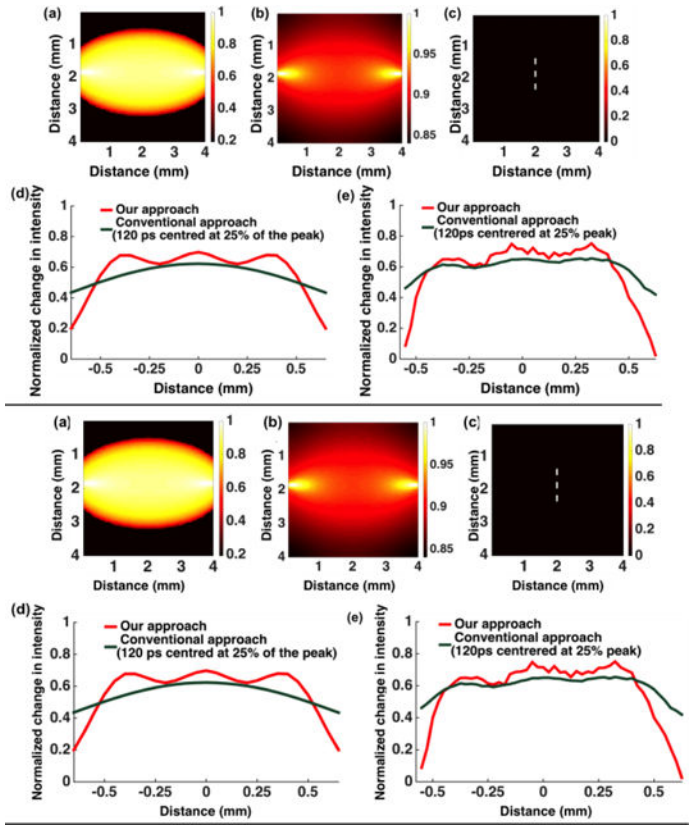

Fig. 3.

Spatial resolution simulation and experimental results. (a, b) Sensitivity profiles of earliest gate photons (a) and conventional early photon gates (b) from a Monte-Carlo simulation, respectively. (c) The simulated 4×4 mm object with three high absorptive regions of 200 × 50 μm separated by 200 μm . (d, e) Source-detector profiles through simulation (d) and phantom (e).